

Single impact crater functions for ion bombardment of silicon

N. Kalyanasundaram, M. Ghazisaeidi, J. B. Freund, and H. T. Johnson^{a)}

Department of Mechanical Science and Engineering, University of Illinois at Urbana-Champaign, Urbana, Illinois 61801, USA

(Received 1 February 2008; accepted 11 March 2008; published online 3 April 2008)

The average effect of a single 500 eV incident argon ion on a silicon surface is studied using molecular dynamics simulations. More than 10^3 ion impacts at random surface points are averaged for each of seven incidence angles, from 0° to 28° off normal, to determine a local surface height change function, or a *crater function*. The crater shapes are mostly determined by mass rearrangement; sputtering has a relatively small effect. Analytical fitting functions are provided for several cases, and may serve as input into kinetic Monte Carlo calculations or stability analyses for surfaces subjected to ion bombardment. © 2008 American Institute of Physics.

[DOI: 10.1063/1.2905297]

Ion bombardment of a solid locally changes the height of the target surface. One of the collective effects of the local surface height change due to individual ion impacts is the so-called sputter-erosion surface instability, which is widely reported to form patterns on semiconductors¹⁻⁹ and other materials.¹⁰⁻¹⁴ Current models of these instabilities rely upon Sigmund's sputtering model¹⁵ and its subsequent extension by Bradley and Harper.¹⁶ In this view, the essential effect of a single incident medium energy (~ 1 keV) ion on an initially flat surface is to remove a volume of material that can be approximately described using a Gaussian distribution centered at the point of impact. This implies that the geometrical effect on the surface is due to sputtering alone. The objective of this study is to investigate atomic-scale mass rearrangement relative to mass removal (sputtering) for single ion impacts. The relative importance of mass rearrangement and sputtering is quantified by the average change in surface height in the neighborhood of the impact point. Atomistic computations of thousands of impacts are used to compute smooth functions representing the mean change in surface height. We call these functions *crater functions*.

Existing sputter-erosion models such as the Bradley-Harper model¹⁶ or the Makeev-Barabasi model¹⁷ use Sigmund's sputtering theory¹⁵ to relate erosion rates to spatial derivatives of the local surface height. These models follow Sigmund's theory and assume that a linear collisional damage cascade due to ion impacts leads to a Gaussian ellipsoid-shaped profile of energy deposition. The energy deposition profile due to an impact at $\mathbf{r}_0 = [x_0, h(x_0, t)]$ is

$$E(\mathbf{r}) = \frac{\varepsilon}{(2\pi)^{3/2} \sigma \mu^2} \exp \left[-\frac{(h - h_0 - a_p)^2}{2\sigma^2} - \frac{(x_1 - x_{01})^2 + (x_2 - x_{02})^2}{2\mu^2} \right], \quad (1)$$

where $E(\mathbf{r})$ is the total energy available due to the ion impact at $\mathbf{r} = [x, h(x, t)]$, $\mathbf{x} = (x_1, x_2)$, $h = h(\mathbf{x}, t)$, and $h_0 = h(x_0, t)$, ε is the energy of an incident ion, a_p is the penetration depth, and σ and μ represent material-dependent widths of the energy distribution. For off-normal beam incidence angles, x_1 is along the projected direction of ion impacts. Bradley and

Harper¹⁶ propose a mechanism whereby height change at any point on the surface is by sputtering, which is proportional to the total energy at that point. Effectively, the change in surface height due to a single ion impact is assumed to be proportional to a Gaussian-shaped function and the net change in surface height is such that

$$\frac{\partial h}{\partial t} \propto \int \int d\mathbf{r} E(\mathbf{r}) \Phi(\mathbf{r}), \quad (2)$$

where $\Phi(\mathbf{r})$ is a geometric correction to the uniform flux J due to surface curvature. The collision cascade approach that is often associated with this energy deposition profile is applicable for higher impact energies and is not necessarily useful in the ≈ 1 keV range in which it is commonly applied.

The applicability of the Sigmund-based Bradley-Harper mechanism for modeling the sputter-erosion surface instability is a topic of current discussion. Several studies^{1,10,18} invoke this mechanism to attempt to explain the dependence of ripple wavelength on temperature and flux, but these explanations of the experimental observations are incomplete. In addition to sputtering, transport along the surface has also been suggested to be important, either for roughening¹⁹ or

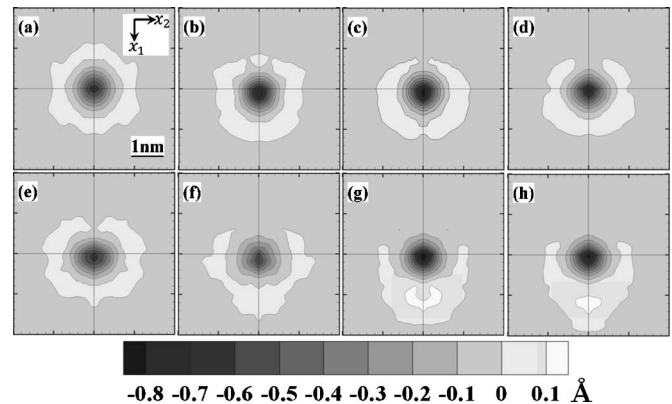


FIG. 1. Crater functions for 500 eV single argon ion impacts on silicon, for incidence angles (a) $\theta = 0^\circ$ (2048 ensembles), (b) $\theta = 4^\circ$ (1026 ensembles), (c) $\theta = 8^\circ$ (1026 ensembles), (d) $\theta = 12^\circ$ (1026 ensembles), (e) $\theta = 16^\circ$ (1026 ensembles), (f) $\theta = 20^\circ$ (1026 ensembles), (g) $\theta = 24^\circ$ (506 ensembles), and (h) $\theta = 28^\circ$ (506 ensembles). For the $\theta > 0^\circ$ cases, the ion motion parallel to the surface is in the x_1 direction, from top to bottom in the orientation of the plots as shown. The thin lines intersect at the point of impact.

^{a)}Electronic mail: htj@uiuc.edu.

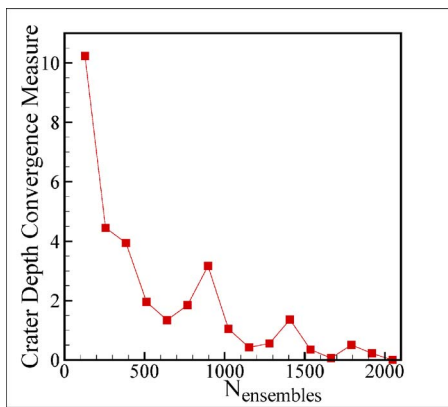


FIG. 2. (Color online) Relative change in computed crater depth with additional ensemble averaging up to 2048 ensembles, for the $\theta=0^\circ$ case, showing approximate convergence of the statistical data.

smoothing.^{19,20} Using simplified molecular dynamics simulations, Feix *et al.* have observed deviations from the Gaussian-shaped mass removal profiles.²¹ This motivates the present study of the geometric effect of an average ion impact on the target surface and our critical assessment of the implied Gaussian-shaped material removal profile. Thus, we atomistically compute crater functions by ensemble averaging the change of surface heights of many single-ion impacts. The crater function data show the relative role of rearrangement and removal, and it can be used to model long-time surface evolution due to ion bombardment, either numerically using a Monte Carlo type approach,²² or analytically using stability analysis methods,²³ both of which have been recently demonstrated.

Cratering effects for cluster bombardment and for higher energy ion bombardment of other materials, particularly metals and polymers, have been computationally and experimentally studied by previous authors.^{24–28} Single ion impacts on silicon are studied in the present work due to the wide use of silicon in the semiconductor industry and because sputter erosion of silicon surfaces has been widely experimentally studied. Sub-keV argon ion beams are frequently used in mild surface modification processes, plasma processing of semiconductors, and in creating surface patterns. Due to the technological relevance of the argon-silicon combination, and to contribute to a potential understanding of the sputter-erosion surface instability in silicon, we consider argon impacts on silicon at 500 eV beam energies and a range of beam incidence angles.

The change in surface height due to an ion impact depends on the atom positions before and after the ion impact. We track atomic trajectories with standard MD simulations of argon ion bombardment using the Stillinger–Weber potential²⁹ for Si–Si interactions and the Moliere potential³⁰ for Ar–Si and Ar–Ar interactions. The target consists of 8000 silicon atoms arranged in a cubic box approximately 5.43 nm on a side. Time integration is with the velocity-Verlet algorithm. Complete details of the MD simulations methodology used here are presented in a prior study.³¹

It has been shown that low temperature 500 eV ion bombardment makes an initially crystalline target essentially amorphous for a fluence of only 2.0×10^{14} ions/cm²,³¹ which is on the order of seconds under typical experimental conditions. Thus, most ions in typical experiments impact an amorphous surface, so we prepare the surface in our simulations to match these expected conditions by first simulating 500 eV ion bombardment of an initially crystalline target up to a fluence of 4.0×10^{14} ions/cm².

Single 500 eV ions are then made to impact random points \mathbf{x}_0 on the surface at prescribed incidence angles. The surface shape before and after an impact is based on the zero-force position of a virtual silicon probe atom.³² These surface heights are computed in a 21×21 mesh of data “bins” overlaying the 5.43×5.43 nm² surface. The change in surface height data is then averaged over 500 to 2000 impacts for each incident angle θ , depending upon the number of ensembles needed to converge statistics at each angle. The resulting impact crater function, $\Delta h_{\text{ion}}(\mathbf{x}-\mathbf{x}_0, \theta)$, includes changes in surface height due to both sputtering and ion-induced atomic rearrangements.

The impact crater functions for 500 eV argon bombardment of silicon at eight local incidence angles are shown in Fig. 1. Since the in-plane projected direction of ion incidence is the x_1 direction, the surface height change, shown as the contour variable, is also averaged across the symmetry axis. The relative convergence of the crater depth for normal incidence as a function of number of ensembles is shown in Fig. 2. Fine details of the crater shapes may be smoothed by additional averaging or may be sensitive to the particular choice of empirical interatomic potentials, but the main features that emerge are unambiguous. Given the small scale of the vertical (contour) coordinate, the small noise that appears in each contour plot is considered insignificant. No single ion impact is expected to yield the surface changes shown in Fig. 1, but these averaged profiles provide a clear picture of the mean effects of the ions.

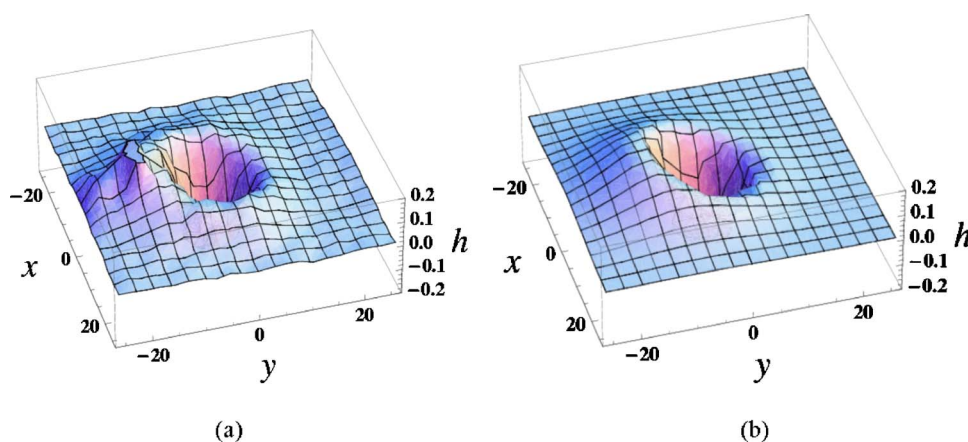


FIG. 3. (Color online) Comparison between the computed crater function and (a) the fitted crater function [Eq. (3)] for the 28° angle of incidence case. All dimensions are in angstrom.

TABLE I. Analytical fitting parameters for three angles of incidence.

	0°	16°	28°
a_1 (Å)	0.205	0.169	0.201
σ_1 (Å ⁻²)	0.005 53	0.00520	0.005 31
b_1 (Å)	7.46
a_2 (Å)	0.805	0.788	0.891
σ_2 (Å ⁻²)	0.0315	0.0325	0.0357
b_2 (Å)	...	1.20	1.48

The key qualitative difference from the Sigmund-based sputter-erosion model is that impacts on average create regions of both reduced and increased surface height, or crater and crater rim, respectively. For the case of normal incidence [Fig. 1(a)], we observe only small deviations from axisymmetry due to the finite number of samples used for statistical averaging. However, as the angle of incidence increases, more material is moved in the projected impact direction, causing a clear asymmetry in the crater rim. For impact angles greater than $\theta=16^\circ$, there is material pileup in the projected ion direction and corresponding opening of the crater rim in the opposite direction. The central crater shape is relatively insensitive to incidence angle.

The presence of crater rims clearly indicates that mass is rearranged by the ion impact and the volume of the crater is much too large to be explained by sputtering alone. Bringa *et al.* have made similar observations on the relation between cratering and sputtering for higher energy single impacts on metallic surfaces.^{26,27} The average number of sputtered silicon atoms per impact for our model system is 0.49,³¹ which accounts for less than 20% of the volume required to create the average crater volume observed here. Instead, the majority of the crater volume is due to material rearrangement required to create the crater rims. We also note that these crater widths, heights, and depths are significantly smaller than the sputter-erosion surface instability patterns that are observed after long bombardment times.⁸

We note that the crater functions can each be conveniently fit with relatively few parameters, following a simple analytical form given by

$$h = a_1 \exp\{-\sigma_1[x^2 + (y + b_1)^2]\} - a_2 \exp\{-\sigma_2[x^2 + (y + b_2)^2]\}, \quad (3)$$

where $h(x, y)$ is the surface height as a function of position x , the projected ion direction, and y relative to the point of impact. Figure 3 shows the fitted $h(x, y)$ for the 28° crater function, compared with the computational data, where the fitting constants are presented in Table I. This simple functional form fits the computed crater functions to within $\frac{1}{3}$ of the crater rim height pointwise over the entire space. A closer fit is not practical given that the variation in the data is mostly short wavelength noise due to limited statistics.

In summary, we report crater functions for medium energy argon ion bombardment of silicon, which show the significance of local atom rearrangement on the surface height

change due to the effects of the incident ions; height change due to atom rearrangement is far greater than due to sputtering alone. Thus, mass rearrangement and not sputtering alone should be considered in accounting for ripple or dot formation on ion-bombarded surfaces. The crater functions we compute have a smooth dependence on incidence angle. For use in models of surface evolution, the crater shapes have been fitted with simple analytical functions.

This work was supported by National Science Foundation Grant No. CMS-0510624.

- ¹J. Erlebacher, M. J. Aziz, E. Chason, M. B. Sinclair, and J. A. Floro, *Phys. Rev. Lett.* **82**, 2330 (1999).
- ²R. Gago, L. Vazquez, R. Cuerno, M. Varela, C. Ballesteros, and J. M. Albella, *Nanotechnology* **13**, 304 (2002).
- ³F. Frost, A. Schindler, and F. Bigl, *Phys. Rev. Lett.* **85**, 4116 (2000).
- ⁴C. Hofer, S. Abermann, C. Teichert, T. Bobek, H. Kurz, K. Lyutovich, and E. Kasper, *Nucl. Instrum. Methods Phys. Res. B* **216**, 178 (2004).
- ⁵S. Ichim and M. J. Aziz, *J. Vac. Sci. Technol. B* **23**, 1068 (2005).
- ⁶S. Fackso, T. Dekorsky, C. Koerdt, C. Trappe, H. Kurz, A. Vogt, and H. L. Hartnagel, *Science* **285**, 1551 (1999).
- ⁷S. J. Chey, J. E. V. Nostrand, and D. G. Cahill, *Phys. Rev. B* **52**, 16696 (1995).
- ⁸B. Ziberi, F. Frost, T. Höche, and B. Rauschenbach, *Phys. Rev. B* **72**, 235310 (2005).
- ⁹G. Ozaydin, A. S. Ozcan, Y. Wang, K. F. Ludwig, H. Zhou, R. L. Headrick, and D. P. Siddons, *Appl. Phys. Lett.* **87**, 163104 (2005).
- ¹⁰W. L. Chan and E. Chason, *Phys. Rev. B* **72**, 165418 (2005).
- ¹¹V. Shulga, *Nucl. Instrum. Methods Phys. Res. B* **174**, 423 (2001).
- ¹²X. Hu, D. G. Cahill, and R. S. Averback, *Appl. Phys. Lett.* **76**, 3125 (2000).
- ¹³S. Rusponi, C. Boragno, and U. Valbusa, *Phys. Rev. Lett.* **78**, 2795 (1997).
- ¹⁴T. M. Mayer, E. Chason, and A. J. Howard, *J. Appl. Phys.* **76**, 1633 (1994).
- ¹⁵P. Sigmund, *Phys. Rev.* **184**, 383 (1969).
- ¹⁶R. M. Bradley and J. M. E. Harper, *J. Vac. Sci. Technol. A* **6**, 2390 (1988).
- ¹⁷M. A. Makeev, R. Cuerno, and A.-L. Barabasi, *Nucl. Instrum. Methods Phys. Res. B* **197**, 185 (2002).
- ¹⁸J. Erlebacher, M. J. Aziz, E. Chason, M. B. Sinclair, and J. A. Floro, *J. Vac. Sci. Technol. A* **18**, 115 (2000).
- ¹⁹G. Carter and V. Vishnyakov, *Phys. Rev. B* **54**, 17647 (1996).
- ²⁰M. Moseler, P. Gumbsch, C. Casiraghi, A. C. Ferrari, and J. Robertson, *Science* **309**, 1545 (2005).
- ²¹M. Feix, A. K. Hartmann, R. Kree, J. Munoz-Garcia, and R. Cuerno, *Phys. Rev. B* **71**, 125407 (2005).
- ²²E. Chason, W. L. Chan, and M. S. Barathi, *Phys. Rev. B* **74**, 224103 (2006).
- ²³B. Davidovitch, M. J. Aziz, and M. P. Brenner, *Phys. Rev. B* **76**, 205420 (2007).
- ²⁴K. Nordlund, J. Keinonen, M. Ghaly, and R. S. Averback, *Nucl. Instrum. Methods Phys. Res. B* **148**, 74 (1998).
- ²⁵X. Hu, K. Albe, and R. S. Averback, *J. Appl. Phys.* **88**, 49 (2000).
- ²⁶E. M. Bringa, R. E. Johnson, and R. M. Papaleo, *Phys. Rev. B* **65**, 094113 (2001).
- ²⁷E. M. Bringa, J. Keinonen, and K. Nordlund, *Phys. Rev. B* **64**, 235426 (2001).
- ²⁸R. M. Papaleo, L. S. Farenzena, M. A. de Araujo, R. P. Livi, M. Alurralde, and B. Bermudez, *Nucl. Instrum. Methods Phys. Res. B* **148**, 126 (1999).
- ²⁹F. Stillingner and T. Weber, *Phys. Rev. B* **31**, 5262 (1985).
- ³⁰V. G. Moliere, *Z. Naturforsch. A* **2A**, 133 (1947).
- ³¹M. C. Moore, N. Kalyanasundaram, J. B. Freund, and H. T. Johnson, *Nucl. Instrum. Methods Phys. Res. B* **225**, 241 (2004).
- ³²N. Kalyanasundaram, J. B. Freund, and H. T. Johnson, *ASME J. Eng. Mater. Technol.* **127**, 457 (2005).